Segmentation by Data Point Classification Applied to Forearm Surface EMG

Jonathan Feng-Shun Lin[1(✉)], Ali-Akbar Samadani[2], and Dana Kulić[1]

[1] Department of Electrical and Computer Engineering, University of Waterloo, Waterloo, ON, Canada
{jf2lin,dkulic}@uwaterloo.ca
[2] Institute of Biomaterials and Biomedical Engineering, University of Toronto, Toronto, Canada
ali.samadani@utoronto.ca

Abstract. Recent advances in wearable technologies have led to the development of new modalities for human-machine interaction such as gesture-based interaction via surface electromyograph (EMG). An important challenge when performing EMG gesture recognition is to temporally segment the individual gestures from continuously recorded time-series data. This paper proposes an approach for EMG data segmentation, by formulating the segmentation problem as a classification task, where a classifier is used to label each data point as either a segment point or a non-segment point. The proposed EMG segmentation approach is used to recognize 9 hand gestures from forearm EMG data of 10 participants and a balanced accuracy of 83 % is achieved.

Keywords: Motion segmentation · Surface electromyography · Classifiers · Pattern recognition

1 Introduction

Electromyography (EMG), the measure of electrical impulses in the muscles, is a promising approach for gesture recognition [1–3]. In order to utilize EMG-based gesture recognition in naturalistic interactions, the start and end of each gesture must be accurately identified from continuous EMG data; this problem is known as *temporal segmentation*. Segmentation is useful to fields such as human-machine interaction as it breaks down a sequence of complex movements, which may include repetitions of the same gesture, into smaller units, termed *primitives*.

Traditional activity recognition and segmentation techniques employ camera-based systems [4], hand-held inertial measurement units (IMUs) [2] or data gloves [5], but they may not be the most suitable for naturalistic interactions. Camera-based systems require unobstructed line-of-sight, while the form factor of IMUs and data gloves constrict natural hand movements, making them unsuitable for hand gesture recognition. With EMG-based systems, since the electrical impulses

A. Leon-Garcia et al. (Eds.): Smart City 2015, LNICST 166, pp. 153–165, 2016.
DOI: 10.1007/978-3-319-33681-7_13

that control hand movements flow through the forearm, forearm EMG can be used to detect hand and finger movements [6]. The EMG sensors are placed on the forearm and not the hand, so this approach does not impede finger movement or the performance of any hand gestures, allowing for more natural interactions.

However, EMG data suffers from some key difficulties: (1) EMG signal amplitude is a function of neuronal and tissue conductivity [7]; (2) Water and body fat introduces noise that attenuates the EMG signal [7]; (3) Sensor placement must be consistent between participants for comparison studies; and (4) EMG signals should be normalized to minimize inter-participant variability [8].

Due to these difficulties, to date, EMG has received less attention in the literature on activity segmentation and recognition. Many existing works use manual or semi-automated segmentation to isolate motions of interest, and focus on the classification of the isolated waveforms. In these papers, the segmentation is performed by thresholding on the signal envelope [3], instantaneous energy [2], transient energy [9], root mean square (RMS) [10], ratio of auto-regression parameters [11], and standard deviation [1], or the data is assumed to be pre-segmented [12,13]. Other activity recognition papers produce a class label using a sliding window [6,14]. In activity recognition survey papers, EMG-based activity recognition is either only briefly mentioned [15], or omitted [16], emphasizing the lack of research efforts in this field. However, to the authors' best knowledge, no published work has reported temporal results for temporal segmentation based on surface EMG. Kaur *et al.* [17] applied heuristics and wavelet analysis to needle transducer EMG to isolate action potentials in biceps, but only reported the number of action potential segments denoted by the algorithm and not the temporal accuracy of their algorithm. Carrino *et al.* [18] designed an EMG-based system where the user activates a hand gesture recognition system by first flexing the triceps, then performs the hand gesture. Both the triceps flex and the hand gesture are recognized by linear discriminant analysis. This approach is similar to the work proposed in this paper, but does not report the segmentation accuracy.

This paper explores the efficacy of using EMG signals for detecting the start and the end of hand gestures. To this end, an EMG signal is represented in terms of time and frequency meta-features, and a classifier-based segmentation method [19] is used to detect the start and the end of the active region of the EMG signal. The active region of the EMG signal corresponds to the interval within which a hand gesture is performed. The proposed method classifies individual data points as a *segment point* (p_1) or a *non-segment point* (p_0), and has previously been applied to lower-body [19] joint angle data. This segmentation approach is on-line and generalizes across individuals, using only simple signal preprocessing [19]. In this paper, the classifier-based segmentation method is applied to segment motion data based on associated EMG activities measured from the forearm during the continuous production of hand gestures.

2 Proposed Approach

This paper applies a classifier-based time-series segmentation approach [19] to discriminate between forearm EMG samples corresponding to p_1 (segment) and

p_0 (non-segment) classes. However, using classifiers in this manner to perform segmentation raises several issues: (1) Classifiers do not inherently consider temporal information, which is an important aspect of movement data, (2) appropriate generation of training points is also important, as manually labelled segments typically only specify a single time point to denote the start and the end of a given exemplar, which is not suitable for classifiers, as there is minimum difference between the data point at time t_n and at time $t_{n\pm1}$, and (3) unbalanced p_1 and p_0 data samples. These issues are addressed by employing normalization, manual segment point expansion, input vector stacking and downsampling.

Consideration must also be given for the intrinsic difficulties of utilizing EMG. EMG signals tend to be highly individualistic due to body type and sensor orientation. These issues are addressed by employing normalization, EMG channel remapping, as well as considering EMG features that are channel agnostic or robust against signal noise.

2.1 EMG Features

A large number of typical EMG and signal processing features was examined in order to identify those best suited for segmentation. The features considered were selected due to their prevalence in EMG analysis [7,20], for their ability to extract useful information from a noisy signal, as well as their channel agnostic characteristics to reduce the impact of EMG sensor placement variability. The features examined include RMS EMG, mean absolute value, waveform length, slope sign changes, skewness, kurtosis, channel-pair inner-product, channel-pair angle, RMS ratio and peak-to-peak time between the two most active EMG channels, Hurst exponent, Hjorth parameters, Teager energy, entropy, relative entropy, mutual information, peak frequency, band width, peak width as measured at quarter power point from the peak frequency spectral power, and relative spectral power. These features are computed over moving windows.

The best performing features (See Sect. 3.3) are described below. In the following definitions, $E(t)$ is the raw EMG signal, W_n is the length of the window, t_0, t_1 ... t_n denote entries in the window.

Mean Absolute Value. $MAV = \sum_{t_0}^{t_n} \frac{1}{W_n} |E(t)|$.

The MAV is the sum of the absolute values of the EMG signal over a window, which effectively computes a moving average filter of the EMG signal.

Waveform-Length. $WFL = \sum_{t_0}^{t_n} |\dot{E(t)}|$.

The WFL is the cumulative successive change of the EMG signal over a temporal interval. If a signal fluctuates greatly within a window, WFL is high, while a signal with low WFL does not contain a lot of local variations.

Pairwise Inner-Product. $PIP = E(t)_x \cdot E(t)_y$,
where $E(t)_x$ and $E(t)_y$ refer to specific channels of the EMG. The PIP is calculated by taking the dot product of a moving window between two channels, and captures the interactions between channel-pairs.

Root Mean Square. $RMS = \sqrt{\sum_{t_0}^{t_n} \frac{1}{W_n} E(t)^2}$.

The RMS provides a measure of the signal power.

Teager Energy. $TE = \dot{E}^2(t) - E(t) \cdot \ddot{E}(t)$.

The TE is a local property of the signal, that varies with the amplitude profiles and instantaneous frequency of the signal. TE captures the energy required to generate the signal with various amplitude and frequency specifications. For two signals with similar amplitude profile and different frequency components, the Teager energy returns different values.

2.2 Data Processing

Normalization. The motion exemplars are normalized to reduce the impact of the inter- and intra-participant variability resulting from variations in sensor placement and EMG signal magnitude. For EMG data, a known sync motion is collected for baseline purposes. Sensor placement normalization is carried out by finding the appropriate rotations such that the maxima of the EMG norm of the sync motion are always in a given channel, and applying this rotation to all movements by this participant in a given session.

Magnitude normalization is also important, and a normalization coefficient can be calculated in a variety of different ways: (1) channel-wise normalization, where the coefficient is the maximum magnitude of each channel in each gesture, (2) motion-wise normalization, where the coefficient is the maximum magnitude over all the EMG channels, or (3) participant-wise normalization, where the coefficient is the average of the maximum motion-wise magnitude of different trials of the sync motion. All normalization coefficients are calculated from the absolute value of the raw EMG data.

Manual Segment Point Expansion. Manual segments are required to label the training data and for algorithmic validation. Typical methods to obtain manual segments is by hand annotating the data, by video playback, or via a proxy sensor. For EMG, it can be difficult to determine from the EMG data visually where a primitive begins and ends, so manual segments can be denoted from a secondary sensor, such as from camera data or a data glove. Once the manual segments are created, it is necessary to increase the number of segment training points to balance the training dataset. To this end, an additional n_{exp} points before and after each manually labelled segment point are also labelled as p_1 [19].

Input Vector Stacking. Classifier techniques do not typically consider temporal factors. To consider short term temporal effects, the input vector is stacked, so that a given data point includes data from a few time steps before and after the current data point. That is, $t_{use} = [t_{n-n_{stack}} \cdots t_{n-1}, t_n, t_{n+1} \cdots t_{n+n_{stack}}]$. n_{stack} requires tuning to optimize for the data [19].

Downsampling. In a given dataset, there may be more data points of one class over the other. The number of p_1 and p_0 for each exemplar are noted, and the smallest values are denoted as $p_{1_{min}}$ and $p_{0_{min}}$, respectively. Each exemplar is randomly downsampled without replacement to match $p_{1_{min}}$ and $p_{0_{min}}$, to eliminate the unbalanced dataset.

2.3 Classifier Training and Testing

After the above steps, the individual exemplar features are concatenated into a data matrix, and passed into a two-stage training process, consisting of a dimensionality reduction algorithm and a base classifier. Initial testing showed that, like previous work [19], aggregation techniques such as boosting [21], do not heavily influence accuracy scores. Principal component analysis (PCA) [21] is used for pre-classifier dimensionality reduction on feature sets that produce vectorial datasets, such as the channel-pair inner-product, and is not applied for feature sets that produce scalars. The base classifiers [21] examined are as follows: (1) artificial neural networks (ANN), (2) k-nearest neighbour (k-NN), (3) linear discriminate analysis (LDA), (4) quadratic discriminate analysis (QDA), (5) support vector machine (SVM), and (6) thresholding on magnitude, with the threshold determined by the value that returns the highest training accuracy.

To classify, each set of observation data is processed in a similar fashion as the training data. The input vector is normalized, and n_{stack} is applied. The PCA transformation, as calculated from the training data, is also applied to obtain a low-dimensional representation of the data, if applicable. Unlike the training data, no downsampling is applied to the observation data. For algorithm verification purposes, the ground truth p_1 points are expanded by n_{exp}.

3 Experiments and Results

3.1 Motion Database

The classifiers were trained on a database of 10 participants with a mean age of 26.8 years old, performing 5 repetitions of 9 different hand gesture primitives, denoted as the *individual gesture (IG) dataset*, and tested against separate sequences of continuous motions where the 9 primitives are performed in random order, denoted as the *continuous random (CR) dataset*. For this paper, training data was always drawn from the IG dataset, while testing was always done against the CR dataset. Only 6 of the 10 participants contributed randomized motions sequences. The experiment was approved by the University of Waterloo Research Ethics Board, and consent was obtained from all participants.

A single classifier was created from the different participant and gesture data, and used to test against the observation data to evaluate the classifier's inter-participant and inter-gesture robustness. All processing, implementation, and analysis were done in MATLAB 8.0, along with the LIBSVM Toolbox [22].

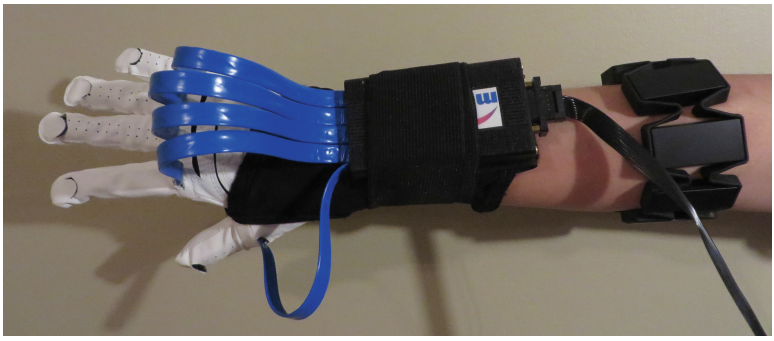

Fig. 1. A participant wearing the Shapehand dataglove from Measurand Inc. (hand and wrist) and the Myo armband from Thalmic Labs Inc. (forearm).

The data was collected by a Myo armband from Thalmic Labs Inc.[1] The EMG armband provides an 8-channel EMG data stream. The armband was placed on the working forearm of the participant, without any specific instructions on armband location or orientation. No conductive paste or other physical attachment site preparation are required when using the Myo. The motion was also collected by a Shapehand dataglove from Measurand Inc.[2] The dataglove provides 15-channel joint angle data, corresponding to each joint in the fingers (Fig. 1). Manual segments were generated by hand annotation on the dataglove data.

The gestures performed were: fist, finger spread, gun, pointing with index finger, pointing with index and middle finger, paddle in, paddle out, snap and thumb-pinky touch. No specific directions on how to perform each motion were given to the participants, so some inter-participant variabilities were observed in how each gesture was executed. Paddle out was used as the sync motion.

3.2 Verification

To calculate the segmentation accuracy, each point in the observation sequence is labelled p_1 or p_0. The number of correctly identified p_1, the true positives (TP), as well as true negatives (TN), false positives (FP), and false negatives (FN), are aggregated together and reported as the balanced accuracy Acc_{Bal}:

$$Acc_{Bal} = \frac{1}{2} \cdot \frac{TP}{TP + FN} + \frac{1}{2} \cdot \frac{TN}{TN + FP}$$

This metric serves as a measure that aggregates both sensitivity and specificity and limits inflated accuracy scores in imbalanced dataset cases.

[1] Thalmic Labs Inc., www.thalmic.com.
[2] Measurand Inc., www.shapehand.com.

3.3 Evaluation of Pre-processing Parameters

In this section, the impact of pre-processing parameters on classification accuracy is examined. The thresholding classifier was selected for this experiment as it is the most common current approach [1,3,10]. The window length is generally smaller than during previous experiments [19], so n_{exp} was set to 5. Larger n_{stack} values improve accuracy, so n_{stack} was kept at 15 [19] to balance between runtime and accuracy. Two factors were examined: (1) EMG features: The EMG features specified in Sect. 2.1 were considered. The calculations were performed over a sliding window of length 20 samples (0.067 s) with a window overlap of 10 samples (0.033 s), (2) normalization type: The different normalization methods specified in Sect. 2.2 were considered.

The influence of these factors on segmentation accuracy are reported in Table 1. These results were generated by dividing the IG dataset into two folds of 5 participants each and using each fold to train a separate classifier. Both classifiers were tested against the CR dataset, and the averaged accuracy between the two classifiers was calculated. The table reports the top 5 performing features according to segmentation Acc_{Bal}. The top performing features while using the threshold approach were the TE, WFL, MAV, RMS + PIP (RP), and raw EMG + RMS + PIP (RRP). Other features examined generally require larger windows of the EMG data to be available, and are not suitable for the temporal resolution required for segmentation purposes.

Table 1 shows that channel-wise normalization did not perform as well as the other normalizations, while the other three normalization methods showed comparable results. This is likely due to channel-wise normalization de-emphasizing individual channel differences in the EMG data between the different gestures. Similar results between normalized and non-normalized data could indicate that these features are not sensitive to inter-participant differences in the signal, leading to comparable results between the no normalization case and the normalization cases. Although participant-based normalization did not perform the best in Table 1, its performance was comparable to the other normalization types, it requires the least amount of input from the participant while improving robustness to large inter-personal variability, and will be used as the normalization scheme in subsequent sections.

3.4 Classifier Evaluation

The best features from Sect. 3.3 (TE, WFL, MAV, RP, and RPP) were used to evaluate the impact of classifier choice. The algorithm parameters used were:

- PCA: PCs set by scree plot method at 80 %.
- k-NN: $k = [1, 3]$.
- Soft-margin SVM: Kernel functions tested were linear, polynomial, radial.
- Feedforward ANN: Layout tested are $[10], [10, 10], [10, 10, 10]$.
- LDA, QDA, thresholding: Euclidean distance was used.

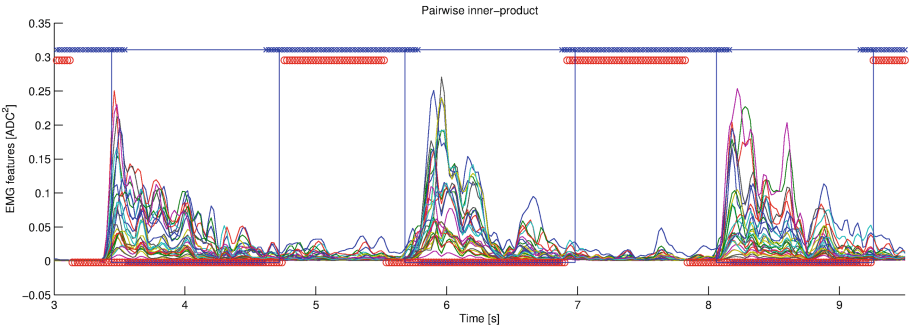

Fig. 2. Segmentation results of a person performing a sequence of random hand gestures, on EMG pairwise inner-product features. The blue rectangles denote the full-motion manual segmentation boundaries. The blue and red lines at the top and bottom denote the classifier p_0 and p_1 for ground truth (blue x) and algorithmic (red circle) segmentation, respectively. (Color figure online)

The results are summarized in Table 2. An illustration of the algorithm segmenting the EMG features can be found in Fig. 2. Similar to Tables 1, 2 was generated by dividing the IG set into two subsets, training a classifier on each subset and averaging the accuracy obtained by each classifier on the testing set. Table 2 shows that ANN and QDA both performed comparatively, showing that both simple and complex classifiers can perform well. In Table 1, the RP was shown to be the best performing feature for participant normalized data, but was outperformed by other features in Table 2.

Table 1. Acc_{bal} scores [%], reported for varying features, after channel, motion, participant or no normalization. The features reported are the top performing features, and are as follows: the Teager energy (TE), waveform-length (WFL), mean absolute value (MAV), the combined features of RMS EMG + inner-product (RP), and the combined features of raw EMG + RMS EMG + inner-product (RRP). Highest Acc_{bal} in each normalization type is bolded. The threshold classifier was used to generate this table, with $n_{exp} = 5$.

	Normalization			
Features	Channel	Motion	Participant	None
TE	72.4 ± 4	74.4 ± 1	73.7 ± 1	73.9 ± 1
WFL	71.6 ± 7	76.2 ± 3	75.3 ± 2	75.6 ± 3
MAV	65.3 ± 12	70.5 ± 8	69.3 ± 9	69.4 ± 9
RP	**73.2 ± 5**	**79.0 ± 0**	**78.2 ± 1**	**78.2 ± 0**
RRP	72.4 ± 1	72.4 ± 1	72.4 ± 1	78.0 ± 0

Table 2. Acc_{bal} scores [%], reported for varying classifiers and features. Top scoring classifier from each classifier type is reported. The best performing features are mean absolute value (MAV), and the RMS + inner-product (RP).

Rank	Classifier	Feature	Accuracy
1	ANN, 10^2	MAV	83 ± 6
2	QDA	MAV	81 ± 7
3	SVM, linear	WFL	81 ± 5
4	LDA	RP	80 ± 6
5	k-NN, 3	MAV	78 ± 7
6	Threshold	RP	78 ± 9

3.5 Leave-One-Gesture-Out Analysis

Table 3 reports the inter-gesture generalization results, where the gesture under inspection was left out of the IG dataset using leave-one-gesture-out (LOGO) cross validation. The training data was generated from the same participant as the observation data, and the Acc_{bal} scores were averaged across all participants. The best performing classifier from Table 2, the ANN, was used for this test.

From Table 3, it can be observed that all features tend to perform similarly, with the exception of RRP. Of all the assessed features, RRP contains 44 (8 from raw EMG, 8 from RMS EMG and 28 from the PIP) elements, which is the largest number of elements. The PCA reduction of RRP features might have resulted in overfitting of training data.

Table 3 also provides insight into the generalizability of the proposed approach to unseen motions. Table 3 suggests that the classifier is able to generalize to most new motions. This is a major potential advantage of the proposed approach, eliminating the need for having a fixed set of *a priori* specified motions. However, some motions, such as the fist motion, do not generalize well, and would need to be explicitly included in the training set to improve the segmentation performance.

3.6 Leave-One-Participant-Out Analysis

To evaluate the generalizability of the learned classifier to participants unseen during training, Table 4 was generated by leaving one-participant-out (LOPO) of the training IG dataset, and testing against the data of that individual from the CR dataset. This cross-validation shows that, for most participants, excellent generalization performance is achieved, with classification results comparable to the case when their data is included in the training set. However, for some participants, *e.g.*, participant 9, lower accuracy scores are observed when they are left out, suggesting that their EMG data differs from the other participants. See Fig. 3 for a comparison between participant 4 and 9. An examination into the movements of participant 9 revealed higher variance in both movement and

Table 3. Acc_{bal} scores [%], reported for LOGO cross-validation. The gestures tested were finger spread (FISP), fist (FIST), gun (GUNM), paddle in (PDIN), paddle out (PDOU), pointing with index finger (POIN), pointing with index and middle (POIM), finger snapping (SNAP) and thumb-pinky touch (THPK). The features listed are the Teager energy (TE), waveform-length (WFL), mean absolute value (MAV), the RMS + inner-product (RP), and the raw EMG + RMS + inner-product (RRP). The ANN classifier was used. The best performing feature for each gesture is bolded.

Gesture	FISP	FIST	GUNM	PDIN	PDOU	POIN	POIM	SNAP	THPK
TE	85 ± 7	77 ± 12	**85 ± 7**	82 ± 11	**87 ± 7**	82 ± 7	82 ± 13	78 ± 5	82 ± 11
WFL	86 ± 6	**76 ± 12**	85 ± 8	**83** ± 11	85 ± 11	**85** ± 8	**86 ± 8**	81 ± 6	**83 ± 10**
MAV	**87** ± 6	76 ± 13	85 ± 8	82 ± 13	83 ± 13	84 ± 10	85 ± 10	**83 ± 6**	82 ± 9
RP	82 ± 9	75 ± 15	85 ± 8	76 ± 12	84 ± 12	85 ± 9	85 ± 9	82 ± 9	81 ± 10
RRP	77 ± 7	69 ± 9	75 ± 8	71 ± 14	78 ± 11	71 ± 9	80 ± 9	70 ± 12	75 ± 9

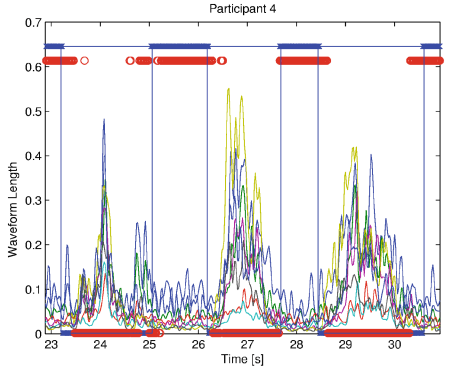

(a) Participant 4, performing pointing with index (23 - 25 sec), pointing with index and middle (26 - 27.5 sec) and paddle out (28.5 - 30.5 sec). This participant obtained a high LOPO score.

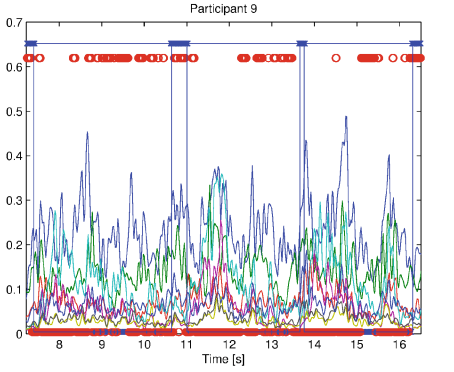

(b) Participant 9, performing 3 instances of pointing with index and middle (7 - 10.5 sec, 11 - 13.5 sec, 14 - 16 sec). Note the dissimilarity between the two participant's motions.

Fig. 3. Segmentation results of two people performing a sequence of random hand gestures, with the WFL feature. The blue rectangles denote the manual segmentation boundaries. The blue and red lines at the top and bottom denote the classifier p_0 and p_1 for ground truth (blue x) and algorithmic (red o) segmentation, respectively. The coloured waveforms correspond to different EMG channels and feature elements. (Color figure online)

resting postures, as well as significant differences in the EMG data between these two participants and the other participants, thus causing a degradation in the segmentation performance. Even when participant 9 is included in the training set, the classifier accuracy does not increase, which suggests differences in which the way the gestures were performed between the IG and the CR data for this participant.

Table 4. Acc_{bal} scores [%], reported for LOPO cross-validation. The features reported are the Teager energy (TE), waveform-length (WFL), mean absolute value (MAV), the RMS + inner-product (RP), and the raw EMG + RMS + inner-product (RRP). The ANN classifier was used. The best performing result for each gesture is bolded.

Participant	4	5	6	7	8	9	10
TE	88 ± 0	87 ± 0	86 ± 1	82 ± 1	83 ± 2	71 ± 4	76 ± 3
WFL	**89 ± 1**	91 ± 1	84 ± 1	82 ± 2	83 ± 1	67 ± 4	**81 ± 1**
MAV	89 ± 1	**91 ± 1**	**86 ± 1**	**83 ± 1**	**87 ± 1**	**72 ± 6**	80 ± 2
RP	88 ± 1	90 ± 0	82 ± 1	82 ± 2	85 ± 2	63 ± 5	78 ± 2
RRP	82 ± 1	83 ± 0	81 ± 1	75 ± 2	71 ± 1	59 ± 3	72 ± 3

From Tables 2, 3 and 4, it is noted that different features achieved the highest balanced accuracy score, suggesting that different combinations of features and classifiers can perform well in different situations. The best feature across all three tables is the MAV, with a 82.9 % with the ANN classifier, 86.5 % with finger spread in the LOGO test, as well as achieving 91.4 % with participant 5 in the LOPO test. This could be due to the fact that the MAV removes the high frequency variations and abrupt changes in the signals, whereas features such as RMS may amplify these fluctuations.

4 Conclusion

This paper shows that EMG serves as an interesting and promising measurement system for gesture segmentation, and that the start and the end of the gestures can be identified from continuously measured EMG data, using a classifier based approach. The proposed segmentation method was shown to generalize across gestures. In many cases, participant generalization was observed as well, but the algorithm is limited by inter-participant variances of muscle activity, resulting in differences in the EMG. The proposed method is capable of on-line segmentation, requiring only an observation window of 0.06 s. Various configurations were tested, such as varying normalization methods or classifier combinations, and revealed that the artificial neural network with the moving averaging feature performed best, achieving a balanced segmentation accuracy of 83 %.

For future work, more sophisticated classifiers that aggregate different classifiers and features together will be investigated, to take advantage of the strength of different classifier-feature combinations. An examination of the data shows that a participant is typically in one of three states: resting, gesture onset, and gesture hold. A multi-class segmentation may be able to improve upon the existing p_0/p_1 approach.

Acknowledgement. The authors of this work would like to acknowledge Thalmic Labs Inc. for providing the Myo armband and the data collection codebase. The authors would also like to acknowledge Dr. Pedram Ataee and the Machine Learning team at Thalmic Labs Inc. for their assistance and insights.

References

1. Costanza, E., Inverso, S., Allen, R.: Toward subtle intimate interfaces for mobile devices using an EMG controller. In: SIGCHI, pp. 481–489 (2005)
2. Zhang, X., Chen, X., Li, Y., Lantz, V., Wang, K., Yang, J.: A framework for hand gesture recognition based on accelerometer and EMG sensors. IEEE Trans. Syst. Man Cybern. A **41**, 1064–1076 (2011)
3. Samadani, A., Kulić, D.: Hand gesture recognition based on surface electromyography. In: EMBC, pp. 4196–4199 (2014)
4. Erol, A., Bebis, G., Nicolescu, M., Boyle, R., Twombly, X.: Vision-based hand pose estimation: a review. Comput. Vis. Image Underst. **108**, 52–73 (2007)
5. Sturman, D., Zeltzer, D.: A survey of Glove-based input. IEEE Comput. Graph Appl. Mag. **14**, 30–39 (1994)
6. Phinyomark, A., Quaine, F., Charbonnier, S., Serviere, C., Tarpin-Bernard, F., Laurillau, Y.: EMG feature evaluation for improving myoelectric pattern recognition robustness. Exp. Syst. Appl. **40**, 4832–4840 (2013)
7. Winter, D., Rau, G., Kadefos, R., Broman, H., De Luca, C.: Units, terms and standards in reporting of EMG research. Electromyogr Kinesiol, Technical report (1980)
8. Oberg, T., Sandsjo, L., Kadefors, R.: Emg mean power frequency: obtaining a reference value. Clin. Biomech. **9**, 253–257 (1994)
9. Chen, Z., Wang, X.: Pattern recognition of number gestures based on a wireless surface EMG system. Biomed. Signal Process. **8**, 184–192 (2013)
10. Kim, J., Mastnik, S., André, E.: Emg-based hand gesture recognition for realtime biosignal interfacing. In: IUI, pp. 30–39 (2008)
11. El Falou, W., Duchêne, J., Hewson, D., Khalil, M., Grabisch, M., Lino, F.: A segmentation approach to long duration surface EMG recordings. J. Electromyogr. Kinesiol. **15**, 111–119 (2005)
12. Naik, G., Kumar, D., Palaniswami, M.: Multi run ICA and surface EMG based signal processing system for recognising hand gestures. In: ICCIT, pp. 700–705 (2008)
13. Ahsan, M., Ibrahimy, M., Khalifa, O.: Electromygraphy (EMG) signal based hand gesture recognition using artificial neural network (ANN). In: ICOM, pp. 1–6 (2011)
14. Yoshikawa, M., Mikawa, M., Tanaka, K.: A myoelectric interface for robotic hand control using support vector machine. In: IROS, pp. 2723–2728 (2007)
15. Chen, L., Hoey, J., Nugent, C., Cook, D., Yu, Z.: Sensor-based activity recognition. IEEE Trans. Syst. Man Cybern. C **42**, 790–808 (2012)
16. Lara, O., Labrador, M.: A survey on human activity recognition using wearable sensors. IEEE Commun. Surv. Tutorials **15**, 1192–1209 (2013)
17. Kaur, G., Arora, A., Jain, V.: Comparison of the techniques used for segmentation of EMG signals. In: MACMESE, pp. 124–129 (2009)
18. Carrino, F., Ridi, A., Mugellini, E., Khaled, O., Ingold, R.: Gesture segmentation and recognition with an EMG-based intimate approach - an accuracy and usability study. In: CISIS, pp. 544–551 (2012)

19. Lin, J., Joukov, V., Kulić, D.: Human motion segmentation by data point classification. In: EMBC, pp. 9–13 (2014)
20. Konrad, P.: The ABC of EMG. Noraxon USA, Technical report (2005)
21. Jain, A., Duin, R., Mao, J.: Statistical pattern recognition: a review. IEEE Trans. Pattern Anal. Mach. Intell. **22**, 4–37 (2000)
22. Chang, C., Lin, C.: LIBSVM: a library for support vector machines. ACM Trans. Intell. Syst. Technol. **2**, 27:1–27:27 (2011)